Polymer Chemistry

Accepted Manuscript

ROYAL SOCIETY OF CHEMISTRY

www.rsc.org/polymers

Polymer Chemistry

RSCPublishing

ARTICLE

A pyridine-flanked diketopyrrolopyrrole (DPP)-based donor-acceptor polymer showing high mobility in ambipolar and n-channel organic thin film transistors

Cite this: DOI: 10.1039/x0xx00000x

Received 00th January 2012,
Accepted 00th January 2012

DOI: 10.1039/x0xx00000x

www.rsc.org/

Bin Sun,[a,b] Wei Hong,[a,b] Hany Aziz[b,c,*] and Yuning Li[a,b,*]

The synthesis and properties of a new polymer semiconductor comprising an electron accepting pyridine-flanked DPP unit and an electron-donating thieno[3,2-*b*]thiophene unit are reported. This polymer has rather low-lying energy levels, which allows transporting both electrons and holes. High crystallinity and a shorter π-π stacking distance of 0.36 nm are achieved due to the strong intermolecular interaction, which are beneficial for charge carrier transport in organic thin film transistors (OTFTs). Well-balanced high electron and hole mobilities up to 3.36 $cm^2V^{-1}s^{-1}$ and 2.65 $cm^2V^{-1}s^{-1}$, respectively, are obtained in top-gate bottom-contact OTFT devices using gold as source and drain contacts. When the contact electrodes are modified with an ultrathin layer (~3 nm) of polyethyleneimine (PEI) to suppress hole injection, unipolar n-type semiconductor performance with high electron mobility of 2.38 $cm^2V^{-1}s^{-1}$ is realized.

Introduction

Organic thin film transistors (OTFTs) are fundamental elements to enable a variety of low-cost, flexible and large area electronics such as flexible displays, radio-frequency identification (RFID) tags, bio-medical sensors, memory devices, etc. [1-5] OTFTs using n-type or p-type organic semiconductors can realize unipolar logic circuits in a similar way as that for the NMOS (n-type metal-oxide semiconductor) or PMOS (p-type metal-oxide semiconductor) technologies, which were developed for the silicon semiconductors. [6] For many applications, the CMOS (complementary metal oxide semiconductor) technology is much more preferred since it offers high switching speed, excellent signal robustness, high noise immunity and low power consumption. [6,7] The greatly improved switching speed in the CMOS circuits is particularly attractive for OTFTs because the carrier mobility of organic semiconductors is still rather low compared to that of the inorganic semiconductors. To fabricate a CMOS-like circuitry, the use of both p-channel and n-channel OTFTs with matching mobilities is mandatory. The high mobility polymers reported to date are predominantly p-type,[8-15] while stable n-type polymer semiconductors[16-23] are much less and the magnitude of the electron mobility is still several factors lower than the hole mobility of p-type polymers. In recent years, ambipolar polymers comprising alternating electron donor (D) and acceptor (A) in their repeat unit have been used as single-component semiconductors to greatly simplify the fabrication process for CMOS-like circuits. [6, 24-29] In these D-A polymers, the donor unit forms hole transporting channels, while the acceptor unit facilitate the electron transport.

Very recently, we reported an ambipolar polymer based on a pyridine-flanked DPP (DBPy) unit as acceptor and a bithiophene as donor, which showed high ambipolar charge transport performance with electron and hole mobilities as high as 6.3 $cm^2V^{-1}s^{-1}$ and 2.78 $cm^2V^{-1}s^{-1}$, respectively.[30] Due to the presence of a less sterically demanding nitrogen atom at the 2-position of pyridine, the DBPy unit is highly coplanar, which is very beneficial for achieving a longer effective conjugation length along the backbone as well as a closer intermolecular π-π stacking distance. In addition, the electron-withdrawing property of pyridine could reduce the lowest unoccupied molecular orbital (LUMO) energy for efficient electron injection and transport. On the other hand, thieno[3,2-*b*]thiophene (TT) has been proven to be an excellent electron donor building block for high mobility polymers, [8, 10, 31, 32] better than bithiophene in some cases, due to its large overlap area for interchain charge carrier hopping. In this study, we synthesized a new D-A polymer by incorporating TT and DBPy units and investigated its optoelectronic properties, molecular ordering, and charge transport performance in ambipolar and n-type OTFTs.

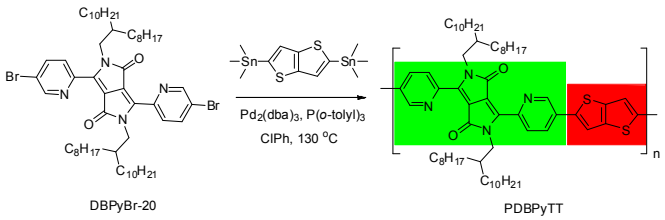

Scheme 1. Synthetic route to PDBPyTT via Stille coupling polymerization.

Results and Discussion

The new D-A polymer PDBPyTT having long branched 2-octyldodecyl side chains was conveniently synthesized via Stille coupling polymerization of the dibromo DBPy co-monomer (DBPyBr-20) [30] with 2,5-bis(trimethylstannyl)-thieno[3,2-*b*]thiophene as shown in Scheme 1. The number average molecular weight (M_n) and the polydispersity index (PDI) of PDBPyTT are 24,500 and 3.00, respectively, which were determined with high-temperature gel-permeation chromatography (HT-GPC) at 140 °C using 1,2,4-trichlorobenzne as an eluent and polystyrene as standards.

The UV-Vis spectrum of PDBPyTT in chloroform solution showed the maximum absorbance at a wavelength of 684 nm (λ_{max}) (Figure 1). The as-cast thin film displayed a slight redshift with a λ_{max} at 690 nm. However, a long wavelength tail has extended to ~1000 nm. The band gap estimated from the absorption onset at ~900 nm is ~1.4 eV. Cyclic voltammetry measurement was used to determine the energy levels of PDBPyTT using ferrocene as a reference, which has a highest occupied molecular orbital (HOMO) energy of -4.8 eV.[33] As shown in Figure 1, a strong reversible oxidative peak was observed. The HOMO level of this polymer was calculated according to the onset oxidation potential to be -5.7 eV. A reversible reduction peak is also seen, but the intensity is very weak. Therefore the LUMO energy level of this polymer was estimated by using the HOMO level obtained by the CV measurement and the optical band gap obtained by the thin film UV-Vis spectrum to be -4.3 eV. These HOMO and LUMO levels are favoured for stable hole (E_{HOMO} < -5 eV)[34] and electron (E_{LUMO} ≤ -4 eV) [16, 35] transport. When Au is used as the source and drain electrodes in an OTFT with PDBPyTT as the channel semiconductor, both the electron and hole injection barriers from Au (with a work function of 4.7-5.1 eV)[36, 37] are quite small. Therefore it was anticipated that PDBPyTT would exhibit ambipolar charge transport behaviour in an OTFT device when Au is used as the source and drain electrodes.

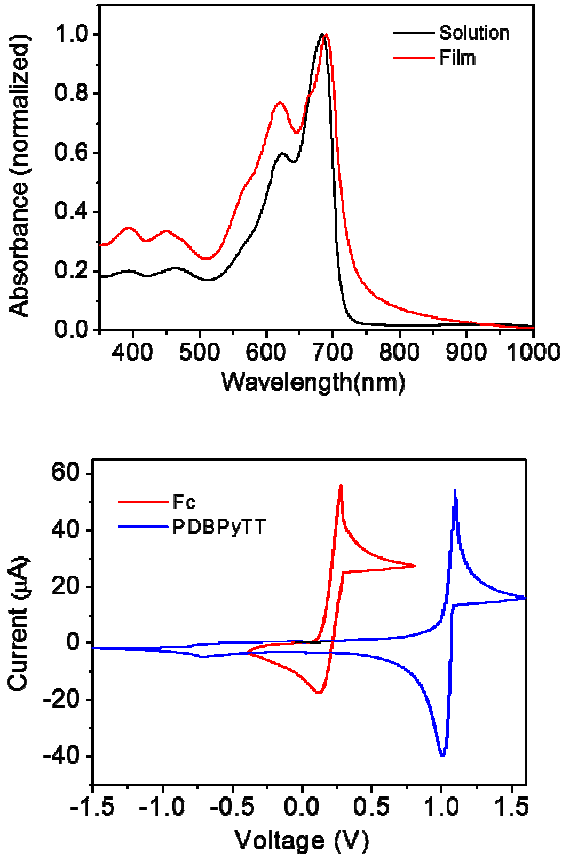

Fig 1. Top: UV-Vis absorption spectra of PDBPyTT solution (chloroform) and as-cast thin film on quartz. Bottom: cyclic voltammetry (CV) curves of PDBPyTT and ferrocene (Fc) (as a reference that has a HOMO level of -4.8 eV)[33] in 0.1 M tetrabutylammonium hexafluorophosphate in anhydrous acetonitrile at a scan rate of 50 mV s^{-1}.

We evaluated the charge transport performance of PDBPyTT in top-gate bottom-contact OTFT devices using Si wafer having a 300 nm-thick insulating SiO_2 layer as the substrate (Figure 2). Au source and drain pairs were thermally deposited on top of the SiO_2 layer using a conventional photolithography technique. A solution of PDBPyTT in chloroform was spin-coated onto the substrate and the resulting polymer thin film (~50 nm) was annealed at a certain temperature in a glove box filled with nitrogen. A Cytop solution was then spin-coated on top of the PDBPyTT layer, followed by baking at 100 °C for 30 min. The thickness of the resulting Cytop dielectric layer is ~570 nm. Finally a ~70 nm-thick Al layer was thermally evaporated on top of the Cytop layer through a shadow mask to complete the device fabrication. The devices were characterized in air in the dark. As expected, all devices showed typical ambipolar charge transport performance (Figure 2 and Table 1). Devices with the 100 °C-annealed PDBPyTT films exhibited electron mobility up to 1.74 $cm^2V^{-1}s^{-1}$ and hole mobility up to 0.35 $cm^2V^{-1}s^{-1}$. For the 150 °C-annealed polymer thin films, the maximum electron and hole mobilities significantly improved to 3.31 $cm^2V^{-1}s^{-1}$ and 2.04 $cm^2V^{-1}s^{-1}$, respectively. When the annealing temperature was increased to 200 °C, the maximum electron mobility slightly improved to 3.36 $cm^2V^{-1}s^{-1}$, but the maximum hole mobility dropped to 1.26 $cm^2V^{-1}s^{-1}$. Figure 3 shows the output and transfer curves of a typical OTFT device with a PDBPyTT film annealed at 150 °C. Based on these device data, it seems that PDBPyTT has similar hole transport performance to, but poorer electron transport capability than the previously reported DBPy-based polymer, PDBPyBT, [30] which comprises a 2,2'-bithiophene donor. The less efficient charge transport property of PDBPyTT is probably due to its less ordered molecular organization as discussed later. PDBPyTT was also tested in a bottom-gate bottom-contact (BGBC) device configuration (ESI). However, hole-only transport with much lower mobilities (~10^{-2} $cm^2V^{-1}s^{-1}$) was obtained, most likely due to the poor interfacial property between the polymer film and the dielectric layer. A similar phenomenon was observed for PDBPyBT.[30]

A previous study demonstrated that even polymer semiconductors that are conventionally considered to be p-type such as regioregular poly(3-hexylthiophene) (P3HT) could show pronounced electron transport behaviour once a low work function metal Ca was used as the source and drain contacts.[38] The high Fermi energy level (E_F) of a low work function conductor can facilitate the electron injection from the electrode to the semiconductor. We thought it would be possible to suppress or eliminate the hole transport characteristics of an ambipolar polymer semiconductor such as PDBPyTT if a low work function conductor is used as the source and drain contacts to create a sufficient energy barrier for blocking hole

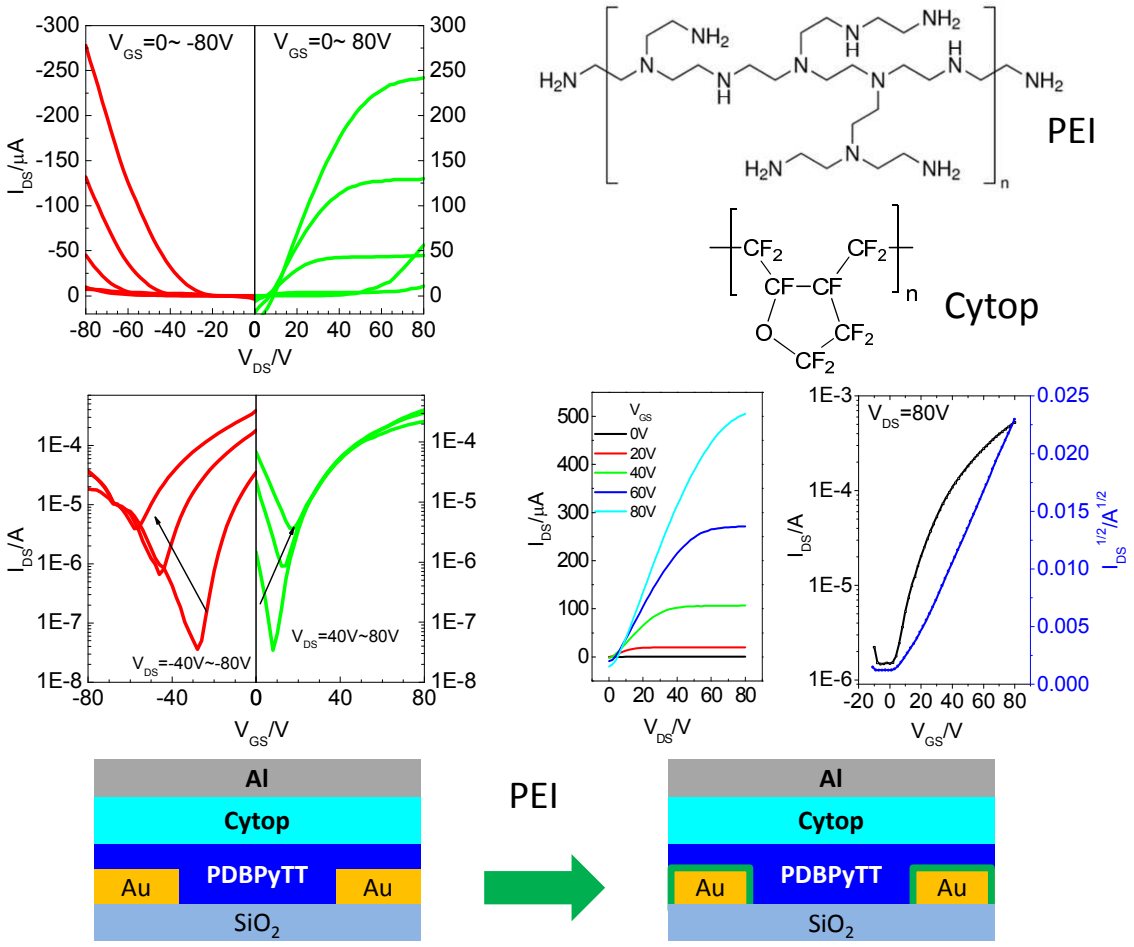

Fig. 2 Left: Output (top) and transfer (middle) curves of a typical ambipolar OTFT device (bottom) under hole and electron enhancement modes; Bottom right: Output (top, left) and transfer (top, right) curves of a typical OTFT device (bottom) with a PEI interlayer (green: ~3.9 nm) between the Au contacts and the PDBPyTT layer; Top right: Chemical structures of PEI and Cytop. The PDBPyTT thin films (~50 nm) in these devices were annealed at 150 °C for 10 min in nitrogen. Device dimensions: channel length L = 30 μm; channel width W =1000 μm.

injection. However, low work function metals such as Ca are generally highly reactive to the moisture and oxygen in air and are not suitable for the fabrication and application of OTFT devices. Recently, a "universal" approach to reducing the work function of conductors was reported by Zhou *et al*.[39] They used air-stable commercially available branched polyethylenimine (PEI) and partially ethoxylated polyethylenimine (PEIE) to modify the conductor surface. The work function of a number of conductor materials could be reduced significantly with an ultrathin PEI or PEIE layer (1-10 nm). This work function reduction effect was accounted for by the molecular dipole moments of the amine groups in these insulating polymers and the charge transfer interaction between the amine groups and the conductor surface. For instance, the work function of the surface-modified Au thin films with PEI and PEIE was reduced to 3.94 eV and 3.90 eV, respectively.[39] This recent finding inspired us to explore the possibility of using this approach to reduce the work function (or increase the Fermi level) of the Au source and drain electrodes to suppress the hole transport characteristic of our ambipolar polymer PDBPyTT in OTFTs. The raised Fermi level of the PEI-modified Au electrodes would build up a large barrier for hole injection from the electrode to PDBPyTT (Figure 3).

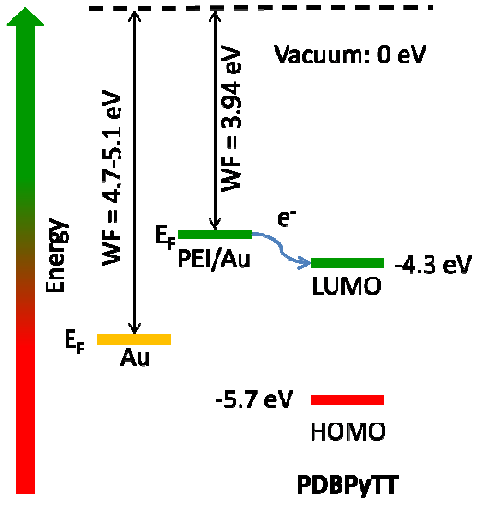

Fig. 3. Energy diagrams of PDBPyTT, Au, and PEI-modified Au, where work function (WF) and E_F are work function and Fermi energy level, respectively. WF values of Au[36, 37] and PEI/Au[39] (PEI modified Au) are from the literature.

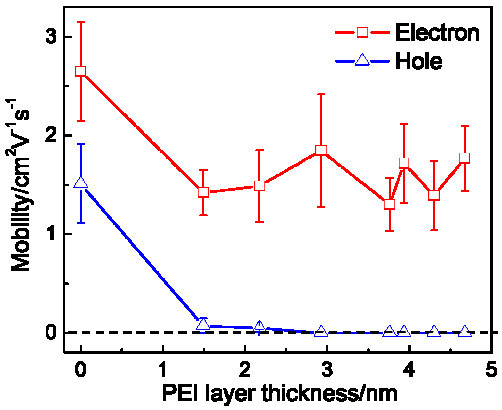

Fig. 4. The dependences of electron and hole mobilities on the PEI layer thickness. Mobility values were obtained from at least 5 OTFT devices for each data point.

We used the similar device configuration as the one for the ambipolar OTFTs except for that a PEI layer on top of the source and drain electrodes (as well as the exposed SiO_2 surface in the channel region) was added (Figure 2). The PEI layer was deposited by spin-coating a PEI solution on the SiO_2/Si substrate pre-patterned with Au source and drain pairs, followed by baking at 100 °C for 10 min, before depositing the PDBPyTT layer. The concentration of PEI was varied to investigate the effect of the PEI layer thickness on the device performance. As can be clearly seen in Figure 4, the average hole mobility dropped precipitously from 1.51 $cm^2V^{-1}s^{-1}$ for the devices without a PEI layer to 0.072 $cm^2V^{-1}s^{-1}$ for the devices with a 1.5 nm-thick PEI layer. When the PEI layer thickness increased to above 2.9 nm, the hole transport characteristic completely vanished and the devices exhibited unipolar n-channel performance. N-channel characteristics of a typical OTFT device with PEI-modified Au electrodes are shown in Figure 2. The average electron mobility is in the range between 1.30 $cm^2V^{-1}s^{-1}$ and 1.89 $cm^2V^{-1}s^{-1}$ for all unipolar n-type OTFT devices with a PEI layer thickness ranging from 2.9 nm to 4.0 nm (Table 1). The highest electron mobility of 2.38 $cm^2V^{-1}s^{-1}$ was achieved for an n-channel device with a 2.9 nm-thick PEI layer. This electron mobility is among the best values for n-type polymer OTFTs reported so far. [16-22] Contact resistance was observed based on the output curves near the origin, which might be due to the poor interfacial property of the semiconductor and the source/drain electrodes resulting from the rough film morphology (see the following AFM images).

To gain insight into the high charge transport performance observed for this new D-A polymer PDBPyTT, we utilized X-ray diffractometry (XRD) technique to examine the polymer chain packing, since the crystal structure has a huge impact on the charge transport performance of polymers.[9] The PDBPyTT thin films spin-coated on SiO_2/Si substrates clearly showed a primary peak at 2θ = 4.23°, which corresponds to a d-spacing of 2.09 nm. A small peak at 2θ = 8.34° is also observed, which is assigned to the secondary reflection peak (Figure 5). These XRD results indicate that the polymer chains in the thin films adopted a layer-by-layer lamellar packing motif, [40] which has been observed for most crystalline conjugated polymers.[9, 15] It is noted that there is no reflection peak around ~20°, which represents the typical π-π stacking distance of ~0.3-0.4 nm. Therefore, the polymer chains in the thin films likely adopted an edge-on packing pattern (Figure 5), which is considered to be most favoured for charge transport in an OTFT device. [41]

To elucidate the π-π stacking distance between polymer main chains, we measured polymer thin films using a transmission XRD mode. As revealed in the diffractogram in Figure 5 (right), a strong peak at 2θ = 11.34° is observed, which is originated from the π–π distance of 0.36 nm. Such a close π–π distance would facilitate the charge hopping through the π–π stacks.

In comparison with the previously reported DBPy polymer, PDBPyBT,[30] PDBPyTT has an identical π–π stacking distance of 0.36 nm. However, the intensity of the primary diffraction peak for the PDBPyTT films is about one order of magnitude

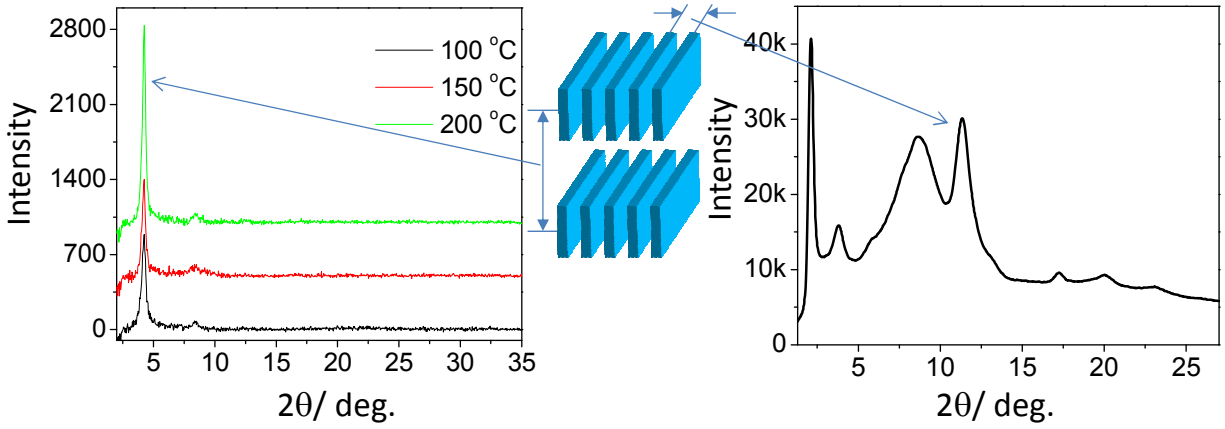

Fig. 5. Left: The reflection XRD diagrams of PDBPyTT thin films (~50 nm thick) spin-coated on SiO2/Si substrates and annealed at difference temperatures using Cu Kα1 radiation (λ = 1.5406 Å). Right: The transmission XRD diagram of a stack of PDBPyTT thin films sandwiched between two Mylar substrates using Mo Kα radiation (λ = 0.71073 Å). The inserted graph in the middle represents the lamellar crystal structure with edge-on chain orientation in the polymer films.

Table 1. Summary of device performance of OTFTs with PDBPyTT.

$T_{annl.}$ [a] °C	Electrode Modification	μ_{e} [b] $cm^2V^{-1}s^{-1}$		μ_{h} [c] $cm^2V^{-1}s^{-1}$		I_{on}/I_{off} [g]	V_{TH} V	*Subthreshold slope* V dec^{-1}
		$\mu_{e,max}$ [d]	$\mu_{e,ave}$ [e] (STD[f])	$\mu_{h,max}$ [d]	$\mu_{h,ave}$ [e] (STD[f])			
100	None	1.74	1.43 (0.35)	0.35	0.28 (0.094)	-	-	-
150	None	3.31	2.65 (0.50)	2.04	1.51 (0.40)	-	-	-
200	None	3.36	3.11 (0.31)	1.26	1.22 (0.049)	-	-	-
150	PEI (4.7nm)	2.14	1.77 (0.33)	-	-	$\sim10^3$-10^4	16	10
	PEI (4.3nm)	1.77	1.39 (0.35)	-	-	$\sim10^2$-10^3	15	18
	PEI (3.9nm)	2.16	1.72 (0.40)	-	-	$\sim10^2$-10^3	12	12
	PEI (3.8nm)	1.61	1.30 (0.27)	-	-	$\sim10^2$-10^3	7	13
	PEI (2.9nm)	2.38	1.85 (0.57)	-	-	$\sim10^3$	5	6
	PEI (2.2nm)	1.82	1.49 (0.36)	0.068	0.05 (0.016)	-	12	-
	PEI (1.5nm)	1.66	1.42 (0.23)	0.20	0.072 (0.076)	-	10	-

a) Annealing temperature; b) Electron mobility measured at V_{DS} = 80 V; c) Hole mobility measured at V_{DS} = -80 V; d) The maximum mobility of the OTFT devices; e) The average mobility obtained from at least five devices; f) The standard deviation; g) Current on to off ratio.

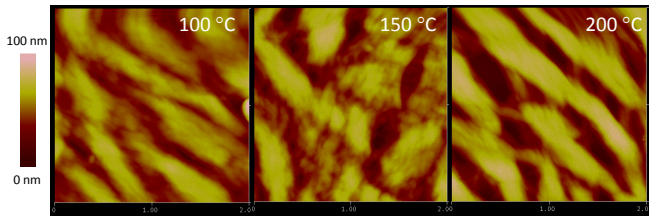

Fig. 6. AFM height images (2 μm × 2 μm each) of PDBPyTT thin films (~50 nm) on SiO_2/Si substrates annealed at different temperatures. Root-mean-square (RMS) roughness: 11.8 nm (100 °C), 14.3 nm (150 °C), and 19.1 nm (200 °C).

weaker than that of the PDBPyBT films having the similar thicknesses. This indicates that the PDBPyTT polymer chains in thin films are substantially less ordered, which results in the poorer charge transport performance of this polymer.

The thin film morphology of PDBPyTT was examined using atomic form microscopy (AFM). For the 100 °C-annealed thin film sample, large domains of ~1 μm × 200 nm were clearly observed and each domain was composed of many small spherical grains (Figure 6). The film has a large root-mean-square (RMS) roughness of 11.8 nm. When the annealing temperature was increased to 150 °C and then 200 °C, the films became even rougher. (The RMS roughness is 14.3 nm for the 150 °C-annealed film and 19.1 nm for the 200 °C-annealed film). The very large crystalline domains present in the polymer thin films might contribute to the high mobility observed for this polymer. However, the large boundaries (or trenches) between domains would be detrimental for charge transport. Optimization of the thin film processing conditions and the side chain design may lead to improved film uniformity and higher crystallinity to enhance the charge transport performance of this polymer.

Conclusions

In summary, we reported a new donor-acceptor polymer semiconductor PDBPyTT comprising an acceptor DBPy unit and a donor thieno[3,2-*b*]thiophene unit, which showed ambipolar charge transport performance with high electron and hole mobilities of 3.36 $cm^2V^{-1}s^{-1}$ and 2.65 $cm^2V^{-1}s^{-1}$, respectively, in OTFT devices with gold source and drain electrodes. The incorporation of thieno[3,2-*b*]thiophene to this polymer resulted in decreased crystallinity of the polymer thin films and thus slightly lower charge transport performance compared with its polymer counterpart containing a bithiophene donor. By simply modifying the source and drain electrodes with a thin layer of PEI, unipolar n-type charge transport characteristics with high electron mobility of 2.38 $cm^2V^{-1}s^{-1}$ was successfully realized for this ambipolar polymer. This polymer is promising as either ambipolar or n-type semiconductor for CMOS-like circuits.

Experimental Section

Materials. 3,6-Di(5-bromopyridin-2-yl)-2,5-bis(2-octyldodecyl) pyrrolo[3,4-*c*]pyrrole-1,4(2*H*,5*H*)-dione (DBPyBr-20) was synthesized according to the previously reported method.[30] All other materials were purchased from commercial sources and used as is.

Instrumentation. UV-Vis spectra were collected on a Thermo Scientific GENESYS™ 10 Spectrophotometer. Reflective XRD spectra were performed on a Bruker D8 Advance powder diffractometer using standard Bragg-Brentano geometry with Cu Kα1 radiation (λ = 1.5406 Å). The polymer thin film (~50 nm thick) samples for the reflective XRD measurements were prepared by spin-coating a polymer solution in chloroform on bare SiO_2/Si substrates and annealed at different temperatures. Transmission XRD measurements were carried out on polymer flakes between two Mylar substrates using Bruker Smart Apex2 CCD with Mo Kα radiation (λ = 0.71073 Å). The atomic force microscopic (AFM) images were obtained on polymer thin films spin-coated on SiO_2/Si substrates using a Dimension 3100 Scanning Probe Microscope. Cyclic voltammetry (CV) measurements of polymer thin films were conducted on a Digi-Ivy DY2111 Potentiostat using a Pt counter electrode, a Pt working electrode and an Ag/AgCl reference electrode in a 0.1 M tetrabutylammonium hexafluorophosphate solution in anhydrous acetonitrile at a scan rate of 50 mV s^{-1}. Ferrocene, which has a HOMO energy level of -4.8 eV,[33] was used as a reference. A Malvern 350 high-temperature gel-permeation chromatography (GPC) system was used to determine the molecular weight of the polymer using 1,2,4-trichlorobenzene as an eluent with polystyrene as standards at a column temperature of 140 °C. The thickness of PDBPyTT and Cytop films were measured using a Dektak 8 Stylus profilometer. The thickness of PEI thin films was measured using a WVASE32

Spectroscopic Ellipsometer by considering a single-layer model (without surface roughness) and Cauchy model fitting.

Synthesis of poly(2,5-bis(2-octyldodecyl)-3,6-di(pyridin-2-yl)-pyrrolo[3,4-*c*]pyrrole-1,4(2*H*,5*H*)-dione-alt-2,5-thieno[3,2-b]thiophene) copolymer (PDBPyTT). To a 50 mL flask were added 3,6-di(5-bromopyridin-2-yl)-2,5-bis(2-octyldodecyl)pyrrolo[3,4-c]pyrrole-1,4(2*H*,5*H*)-dione[30] (0.2018 g, 0.2 mmol), 2,5-bis(trimethylstannyl)thieno[3,2-b]thiophene (0.0932 g, 0.2 mmol) and tri(*o*-totyl)phosphine (5.3 mg, 0.018 mmol). After degassing and filling with argon for 3 times, tris(dibenzylideneacetone)-dipalladium ($Pd_2(dba)_3$) (4.0 mg, 0.0044 mmol) and anhydrous chlorobenzene (20 ml) were added. The mixture was stirred at 130 ºC for 72 h. After cooling down to room temperature, the reaction mixture was poured into methanol (100 mL) under stirring. The precipitated product was filtered off and subjected to Soxhlet extraction with acetone, hexane and then chloroform. The final chloroform extraction was dried to afford the polymer. Yield: 123 mg (62.4 %). GPC: M_n = 24,500, PDI = 3.00; UV-Vis: λ_{max} 684 nm (in chloroform), 690 nm (in thin film). Found: C, 74.2; H, 8.6; N, 5.5; S, 5.7. Calc. for $C_{62}H_{90}N_4O_2S_2$: C, 75.4; H, 9.2; N, 5.7; S, 6.5.

OTFT devices fabrication and characterization. SiO_2/Si wafer patterned with thermally evaporated Au source and drain electrodes with a channel length (L) of 30 μm and a channel width (W) of 1 mm was cleaned with air plasma, rinsed with acetone and isopropanol, and dried with a nitrogen flow prior to device fabrication. Top-gate bottom-contact (TGBC) and bottom-gate bottom-contact (BGBC) OTFT configurations were used to evaluate the polymer semiconductor, where were fabricated as follows.

TGBC OTFTs without electrode modification. A PDBPyTT solution in chloroform (10 mg mL^{-1}) was spin-coated on a cleaned substrate at 2000 rpm for 60 s. The substrate with the deposited polymer film (~50 nm) was annealed on a hotplate at 100, 150, or 200 °C in nitrogen for 10 min. A Cytop layer (~570 nm with Ci = 3.2 nF cm^{-2}) as the gate dielectric was deposited on the polymer semiconductor layer by spin-coating a Cytop solution at 2000 rpm for 60 s, followed by drying on a hotplate at 100 °C for 30 min in nitrogen. Finally, a ~70 nm-thick Al layer was deposited by thermal evaporation as the top gate electrode.

TGBC OTFTs modified with PEI. A PEI (branched polyethylenimine with an average M_w of ~25,000, Sigma Aldrich) solution diluted with isopropanol (in a range of 0.006-0.1 g PEI/100 mL IPA) was spin-coated on a cleaned substrate with patterned source and drain pairs at 5000 rpm for 60 s. After baking on a hotplate at 100 °C for 10 min, a PDBPyTT solution in chloroform (10 mg mL^{-1}) was spin-coated and the polymer film was annealed at 150 °C for 10 min. The Cytop dielectric layer and the Al top gate layer were subsequently deposited as described above.

BGBC OTFTs. The SiO_2/Si substrate was treated with dodecyltrichlorosilane (DDTS) in toluene (10 mg mL^{-1}) at 60 °C for 20 min, followed by washing with toluene and drying under a nitrogen flow. A PDBPyTT film was deposited as above. After annealing on a hotplate in a glove box at 150 or 200 °C for 10 min, the devices were encapsulated with a 500 nm-thick poly(methyl methacrylate) (PMMA) layer by spin coating a PMMA solution (8 wt % in butyl acetate) at 3000 rpm for 60 s, and dried at 80 °C for 30 min under nitrogen. The thermally grown 300 nm-thick SiO_2 dielectric layer has a capacitance of ~11 nFcm^{-2}.

OTFT characterization. The OTFT devices were characterized in air in the absence of light using an Agilent 4155C Semiconductor Parameter Analyzer. The carrier mobility was calculated from the slope of the $(I_{DS})^{1/2}$ versus V_{GS} plot according to the equation, $I_{DS} = \mu C_i W/2L (V_{GS}-V_{TH})^2$, in the saturation regime, where μ is the carrier mobility, I_{DS} is the drain current, L and W are the channel length and channel width, C_i is the gate dielectric layer capacitance per unit area, V_{GS} and V_{TH} are the gate voltage and threshold voltage, respectively.

Acknowledgements

H.A. and Y.L. thank the Natural Sciences and Engineering Research Council (NSERC) of Canada for the financial support (Discovery Grants). The authors thank Drs. Changsheng Wang, David Sparrow, and Steven Tierney of Merck Chemicals Ltd. for the valuable discussions. The authors also thank and Jon Hollinger and Prof. Dwight Seferos of University of Toronto for the measurements of molecular weight and Angstrom Engineering Inc. for providing the thermal deposition system for the fabrication of OTFT devices.

Notes and references

[a] Department of Chemical Engineering,
[b] Waterloo Institute for Nanotechnology (WIN),
[c] Department of Electrical and Computer Engineering, University of Waterloo, 200 University Ave West, Waterloo, ON, N2L 3G1, Canada
*Tel.: +1 519 888 4567 ext. 31105. Fax: +1 519 888 4347. E-mail: yuning.li@uwaterloo.ca; h2aziz@uwaterloo.ca.

† Electronic Supplementary Information (ESI) available

1. C. D. Dimitrakopoulos and P. R. L. Malenfant, *Adv. Mater.*, 2002, **14**, 99.
2. C. Reese, M. Roberts, M.-m. Ling and Z. Bao, *Materials Today*, 2004, **7**, 20.
3. C. Wang, H. Dong, W. Hu, Y. Liu and D. Zhu, *Chem. Rev.*, 2011, **112**, 2208.
4. A. C. Arias, J. D. MacKenzie, I. McCulloch, J. Rivnay and A. Salleo, *Chem. Rev.*, 2010, **110**, 3.
5. H. Klauk, *Chem. Soc. Rev.*, 2010, **39**, 2643.
6. K. J. Baeg, M. Caironi and Y. Y. Noh, *Adv. Mater.*, 2013, **25**, 4210.
7. R. J. Baker, *CMOS: Circuit Design, Layout, and Simulation, 3rd Edition* Tewksbury, S. K., Brewer, J. E., Eds, John Wiley & Sons: Hoboken, NJ, 2010, Chapter 1, pp 6-7.
8. Y. N. Li, S. P. Singh and P. Sonar, *Adv. Mater.*, 2010, **22**, 4862.
9. Y. N. Li, P. Sonar, L. Murphy and W. Hong, *Energy & Environmental Science*, 2013, **6**, 1684.
10. J. Li, Y. Zhao, H. S. Tan, Y. Guo, C.-A. Di, G. Yu, Y. Liu, M. Lin, S. H. Lim, Y. Zhou, H. Su and B. S. Ong, *Sci. Rep.*, 2012, **2**, 754.
11. I. Kang, H.-J. Yun, D. S. Chung, S.-K. Kwon and Y.-H. Kim, *J. Am. Chem. Soc.*, 2013, **135**, 14896.
12. S. Chen, B. Sun, W. Hong, H. Aziz, Y. Meng and Y. Li, *Journal of Materials Chemistry C*, 2014, **2**, 2183.
13. J. Mei, D. H. Kim, A. L. Ayzner, M. F. Toney and Z. Bao, *J. Am. Chem. Soc.*, 2011, **133**, 20130.
14. T. Lei, J. H. Dou and J. Pei, *Adv. Mater.*, 2012, **24**, 6457.
15. C. Guo, W. Hong, H. Aziz and Y. Li, *Reviews in Advanced Sciences and Engineering*, 2012, **1**, 200.
16. H. Yan, Z. Chen, Y. Zheng, C. Newman, J. R. Quinn, F. Dotz, M. Kastler and A. Facchetti, *Nature*, 2009, **457**, 679.
17. Y. Wen and Y. Liu, *Adv. Mater.*, 2010, **22**, 1331.
18. C. Kanimozhi, N. Yaacobi-Gross, K. W. Chou, A. Amassian, T. D. Anthopoulos and S. Patil, *J. Am. Chem. Soc.*, 2012, **134**, 16532.

19. H. Li, F. S. Kim, G. Ren and S. A. Jenekhe, *J. Am. Chem. Soc.*, 2013, **135**, 14920.
20. Z. Q. Yan, B. Sun and Y. N. Li, *Chem. Commun.*, 2013, **49**, 3790.
21. T. Lei, J.-H. Dou, X.-Y. Cao, J.-Y. Wang and J. Pei, *J. Am. Chem. Soc.*, 2013, **135**, 12168.
22. T. Lei, J.-H. Dou, X.-Y. Cao, J.-Y. Wang and J. Pei, *Adv. Mater.*, 2013, **25**, 6589.
23. J. H. Park, E. H. Jung, J. W. Jung and W. H. Jo, *Adv. Mater.*, 2013, **25**, 2583.
24. P. Sonar, S. P. Singh, Y. Li, M. S. Soh and A. Dodabalapur, *Adv. Mater.*, 2010, **22**, 5409.
25. J. D. Yuen, J. Fan, J. Seifter, B. Lim, R. Hufschmid, A. J. Heeger and F. Wudl, *J. Am. Chem. Soc.*, 2011, **133**, 20799.
26. W. Hong, B. Sun, H. Aziz, W. T. Park, Y. Y. Noh and Y. N. Li, *Chem. Commun.*, 2012, **48**, 8413.
27. J. Lee, A. R. Han, H. Yu, T. J. Shin, C. Yang and J. H. Oh, *J. Am. Chem. Soc.*, 2013, **135**, 9540.
28. J. C. Bijleveld, A. P. Zoombelt, S. G. J. Mathijssen, M. M. Wienk, M. Turbiez, D. M. de Leeuw and R. A. J. Janssen, *J. Am. Chem. Soc.*, 2009, **131**, 16616.
29. Z. Chen, M. J. Lee, R. S. Ashraf, Y. Gu, S. Albert-Seifried, M. M. Nielsen, B. Schroeder, T. D. Anthopoulos, M. Heeney, I. McCulloch and H. Sirringhaus, *Adv. Mater.*, 2012, **24**, 647.
30. B. Sun, W. Hong, Z. Yan, H. Aziz and Y. Li, *Adv. Mater.*, 2014, **26**, 2636.
31. I. McCulloch, M. Heeney, C. Bailey, K. Genevicius, I. MacDonald, M. Shkunov, D. Sparrowe, S. Tierney, R. Wagner, W. Zhang, M. L. Chabinyc, R. J. Kline, M. D. McGehee and M. F. Toney, *Nat Mater*, 2006, **5**, 328.
32. Y. Li, Y. Wu, P. Liu, M. Birau, H. Pan and B. S. Ong, *Adv. Mater.*, 2006, **18**, 3029.
33. B. W. D'Andrade, S. Datta, S. R. Forrest, P. Djurovich, E. Polikarpov and M. E. Thompson, *Org. Electron.*, 2005, **6**, 11.
34. B. S. Ong, Y. Wu, P. Liu and S. Gardner, *J. Am. Chem. Soc.*, 2004, **126**, 3378.
35. B. A. Jones, A. Facchetti, M. R. Wasielewski and T. J. Marks, *J. Am. Chem. Soc.*, 2007, **129**, 15259.
36. S. Braun, W. R. Salaneck and M. Fahlman, *Adv. Mater.*, 2009, **21**, 1450.
37. A. Wan, J. Hwang, F. Amy and A. Kahn, *Org. Electron.*, 2005, **6**, 47.
38. L.-L. Chua, J. Zaumseil, J.-F. Chang, E. C. W. Ou, P. K. H. Ho, H. Sirringhaus and R. H. Friend, *Nature*, 2005, **434**, 194.
39. Y. Zhou, C. Fuentes-Hernandez, J. Shim, J. Meyer, A. J. Giordano, H. Li, P. Winget, T. Papadopoulos, H. Cheun, J. Kim, M. Fenoll, A. Dindar, W. Haske, E. Najafabadi, T. M. Khan, H. Sojoudi, S. Barlow, S. Graham, J.-L. Brédas, S. R. Marder, A. Kahn and B. Kippelen, *Science*, 2012, **336**, 327.
40. T.-A. Chen, X. Wu and R. D. Rieke, *J. Am. Chem. Soc.*, 1995, **117**, 233.
41. H. Sirringhaus, P. J. Brown, R. H. Friend, M. M. Nielsen, K. Bechgaard, B. M. W. Langeveld-Voss, A. J. H. Spiering, R. A. J. Janssen, E. W. Meijer, P. Herwig and D. M. de Leeuw, *Nature*, 1999, **401**, 685.

Graphical abstract

A new donor-acceptor polymer based on pyridine-flanked diketopyrrolopyrrole shows high mobilities in both ambipolar and unipolar n-type organic thin film transistors.